Coupled Thermal-fluids-stress Analysis of Castings

Authors: Mark Samonds, Ph.D., J. Z. Zhu, Ph.D.

Affiliation: UES Software Inc., Annapolis, MD, USA

Abstract

This paper will consider some of the issues encountered in the application of a combined eulerian-lagrangian finite element method to shape and continuous castings. The stability and accuracy of thermo-mechanical contact algorithms will be discussed. Appropriate selection of constitutive models for casting alloys and mold materials will be treated, as well as topics concerning fluid-mechanical coupling.

Introduction

The importance and range of applicability of stress analysis in casting simulation has been noted by many authors. Accurate stress results, both in a relative and absolute sense, depend on a number of factors. We will focus on three in particular; 1) use of an appropriate material model, 2) the thermal/mechanical contact algorithm, and 3) issues surrounding the coupling of stress with filling.

Material Models

In order to simulate a variety of materials, several mechanical material models have been adopted in ProCAST. For cast parts and molds, the models include a thermo-elasto-viscoplastic model of the Perzyna type [1], a thermo-elastoplastic counterpart and an elastic model. In addition, a rigid body model and a vacant model are also available for mold materials.

The elastoplastic model and elasto-viscoplastic model, in which all the parameters and functions are temperature dependant, are described in the following. We shall start with the constitutive equations of the elastoplastic model. A modification in the flow rule will lead to the elasto-viscoplastic model.

Elastoplasticity

The rate representation of the total strain in elastoplastic model is given by

$$\dot{\boldsymbol{\varepsilon}} = \dot{\boldsymbol{\varepsilon}}^e + \dot{\boldsymbol{\varepsilon}}^p + \dot{\boldsymbol{\varepsilon}}^T$$

The linear isotropic elastic response is described by

$$\dot{\boldsymbol{\sigma}} = \mathbf{E} : (\dot{\boldsymbol{\varepsilon}} - \dot{\boldsymbol{\varepsilon}}^p - \dot{\boldsymbol{\varepsilon}}^T)$$

Where $\mathbf{E}$ is the elastic constitutive tensor, $\dot{\boldsymbol{\varepsilon}}^e, \dot{\boldsymbol{\varepsilon}}^p, \dot{\boldsymbol{\varepsilon}}^T$ are the elastic strain rate, the plastic strain rate and the thermal strain rate respectively.
A generalized von Mises yield function,

$$f = \sqrt{\frac{3}{2}} \| \mathbf{s} - \mathbf{x} \| - \kappa$$

is used in the numerical computations, where the deviatoric stress is given by

$$\mathbf{s} = \boldsymbol{\sigma} - \frac{1}{3} tr \boldsymbol{\sigma} \mathbf{I}$$

$\mathbf{x}$ is the back stress which controls the kinematic hardening and κ characterizes isotropic hardening.

The assumed plastic flow rule has the form of $\dot{\boldsymbol{\varepsilon}}^p = \gamma \dfrac{\partial f}{\partial \boldsymbol{\sigma}}$, where γ is the plastic multiplier to be determined with the aid of the consistency condition, $f = 0$.

Both *isotropic* and *kinematic* hardening rules are available. For *isotropic hardening*, the rule can be chosen as

$$\kappa = Y_0 + H\bar{\varepsilon}^p$$

where Y_0 is the yield stress and H is the plastic modulus. The effective plastic strain is given by,

$$\bar{\varepsilon}^p = \int_0 \sqrt{\frac{2}{3}\dot{\boldsymbol{\varepsilon}}^p : \dot{\boldsymbol{\varepsilon}}^p}\, d\tau$$

The isotropic hardening rule can also have the form of

$$\kappa = Y_\infty + (Y_0 - Y_\infty)e^{-\alpha\bar{\varepsilon}^p}$$

where Y_∞ is the ultimate stress and α is a material parameter.

For *kinematic hardening*, the Armstrong-Frederick model [2] is adopted and has the form of

$$\dot{\mathbf{x}} = c\dot{\boldsymbol{\varepsilon}}^p - b\dot{\bar{\varepsilon}}^p\mathbf{x}$$

where $\dot{\bar{\varepsilon}}^p = \sqrt{\frac{2}{3}\dot{\boldsymbol{\varepsilon}}^p : \dot{\boldsymbol{\varepsilon}}^p}$ and c and b are material parameters.

Elasto-viscoplasticity

The viscoplastic model has a similar structure as the plastic model described above, except that the flow rule is changed. Here, positive values of the yield function are admitted and for *f* > 0, the plastic multiplier is replaced by a material function.

$$\gamma = \frac{1}{\eta}\phi(f)$$

Therefore, the flow rule has the form

$$\dot{\boldsymbol{\varepsilon}}^p = \frac{1}{\eta}\phi(f)\frac{\partial f}{\partial \boldsymbol{\sigma}}$$

where $\phi(f) = \left\langle \dfrac{f}{Y_0} \right\rangle^m$ and η and m are material constants. The $\langle\ \rangle$ notation means

$$\langle x \rangle = \frac{1}{2}\left(x + |x|\right)$$

The constitutive equations for both the elastoplastic and elasto-viscoplastic models are solved by a Backward-Euler time integration scheme [3], which is unconditionally stable.

Thermal and Mechanical Contact of Casting and Mold

One of the critical aspects of the calculation is the treatment of the interfaces between the casting and mold, considering both thermal and mechanical aspects.

A multi-body mechanical contact algorithm is employed to compute the contact and gap formation between the casting and mold parts. Contacts between different mold parts is also considered. An augmented Lagrangian type method [4] is used in the contact algorithm. An additional automatic penalty number augmentation technique is implemented in the algorithm to adjust the penalty number and thereby the contact force. Such a technique greatly enhances the stability and robustness of the contact computation algorithm.

The variational form of the equilibrium equation with mechanical contact at any time t is written as

$$\int_\Omega \sigma \bullet grad(\delta\mathbf{u})d\Omega - \int_\Omega \mathbf{b} \bullet \delta\mathbf{u}d\Omega - \int_{\Gamma_\sigma} \bar{\mathbf{t}} \bullet \delta\mathbf{u}d\Gamma + \int_{\Gamma_c} \left\langle \lambda^k + \xi g(\mathbf{u}) \right\rangle \mathbf{n} \bullet \delta\mathbf{u}d\Gamma = 0$$

Here a frictionless contact is considered for simplicity. In the above equation, Ω represents the geometry of casting and all the mold parts, Γ represents all the contact interface between all parts. The body forces and surface tractions are denoted by $\mathbf{b}$ and $\mathbf{t}$ respectively.

The quantity $\left\langle \lambda^k + \xi g(\mathbf{u}) \right\rangle$ is the augmented Lagrangian multiplier and ξ is the penalty number.

Thermal contact between parts is considered by adjusting the interface heat transfer coefficient with respect either to the air gap width or the contact pressure as computed by the mechanical contact algorithm. When the gap width is greater than zero, the adjusted heat transfer coefficient has the form,

$$h_{eff} = \cfrac{1}{\cfrac{1}{h_0} + \cfrac{1}{\left(h_{air} + h_{rad}\right)}}$$

where h_0 is the initial value of the heat transfer coefficient

$h_{air} = k_{air}/g$

$k_{air} = $ conductivity of air or 0. for vacuum

$g = $ gap width

$h_{rad} = $ radiation heat transfer coefficient

If the contact pressure is non-zero, the effective heat transfer is increased linearly with that pressure up to a maximum value. This rather simplistic approach will be refined in the future.

Implementation

The casting process is simulated by a coupled thermal-fluid-stress analysis using the finite element method in an eulerian-lagrangian framework. Different types of elements can be used in the finite element discretization [5]. We refer to [6] for details of the elements used in ProCAST as well as the implementation of the numerical algorithms.

A sequential solution strategy, based on operator splitting, is employed in the treatment of the coupled problem. The stress problem is solved by a Newton-Raphson method using a consistent tangent operator. A line search algorithm is adopted to optimize the convergence of the Newton-Raphson iteration. Because of the computational expense, the stress solution may be done at a less frequent interval than the thermal-fluid analysis.

When free surface flow is involved, as in filling, it is of course necessary to skip over the empty elements in the stress analysis. Care also has to be taken in the treatment of the liquid elements. Those elements that are connected by some path to a free surface can also be skipped. The volumetric change in those elements, due to thermal contraction and phase change, will be accounted for by the free surface algorithm. However, those liquid elements that are in a volume enclosed by solid need to be included in the stress calculation because that volumetric change will affect the state of stress in the surrounding elements. For example, a contraction in the liquid elements will result in a tensile stress that can deform a surrounding solid shell.

Numerical Results

The first example demonstrates the importance of using proper material models in the stress analysis. The problem considered is an aluminum casting in a sand mold. The mold material model is chosen as elastoplastic with linear strain hardening. The casting material model is treated with two alternatives, elastic and elasto-viscoplastic. An isotropic linear hardening law is assumed for the elaso-viscoplastic model. The initial temperature of the casting is taken as $650°C$ and the mold temperature as $25°C$. All material data are temperature dependent. The results in Figure 1 show the accumulated plastic strain for both material models. Naturally, with an elastic model for the casting, on the left, the only plastic strain occurs in the mold. Figure 2 depicts the corresponding final effective or von Mises stress. The elastic model results in a maximum stress in the casting more than twice that in the other model. The viscoplastic model can relieve stress through plastic deformation. Thus, if the absolute value of the stress in a casting is desired, it is necessary to utilize one of the nonlinear material models.

In the second example, a simple T shaped casting of A356 in a H13 mold is simulated, as shown in Figure 3. The effective interface heat transfer coefficient at two different points on the casting is plotted in Figure 4. The top curve is from a point experiencing increasing contact pressure as the casting contracts. The middle curve is from a point where a gap is opening up between casting and mold, assuming the presence of air. The bottom curve is from that same point, but assuming a vacuum. The large variation in the coefficient illustrates the importance of accounting for local conditions. In addition, this example illustrates the value of the reverse coupling of the mechanical deformations with the energy solution. This effect can be seen in Figure 4 on the right where the heat flux contours are plotted. The heat flux is greatest where the contact pressure is highest.

The third example is a simple 2D casting, with an insulated riser, that has been specifically designed to produce two fluid regions. One of these is connected to the free surface at the top, which we will call Class 1, and the other becomes enclosed by solid, Class 2. In the result on the left, both Classes of elements are included in the stress analysis at all times, even during filling. In the simulation on the right, the Class 1 elements are not included in the stress calculation until they begin to solidify. The Class 2 elements are included as soon as they are cut off from the riser feeding. This results in a cpu time reduction of approximately 50% and a stress field that is more smooth.

As a practical industrial example, one company was having trouble with cracking in a tilt pouring mold. The simulated results, on the left in Figure 7, showed high stress concentrations exactly where the cracks were appearing. The redesigned mold, on the right in Figure 7, had much lower stress concentrations in the same area and eliminated the cracking problem.

Figure 1: Accumulated Plastic Strain, Elastic Model (left) and Viscoplastic (right)
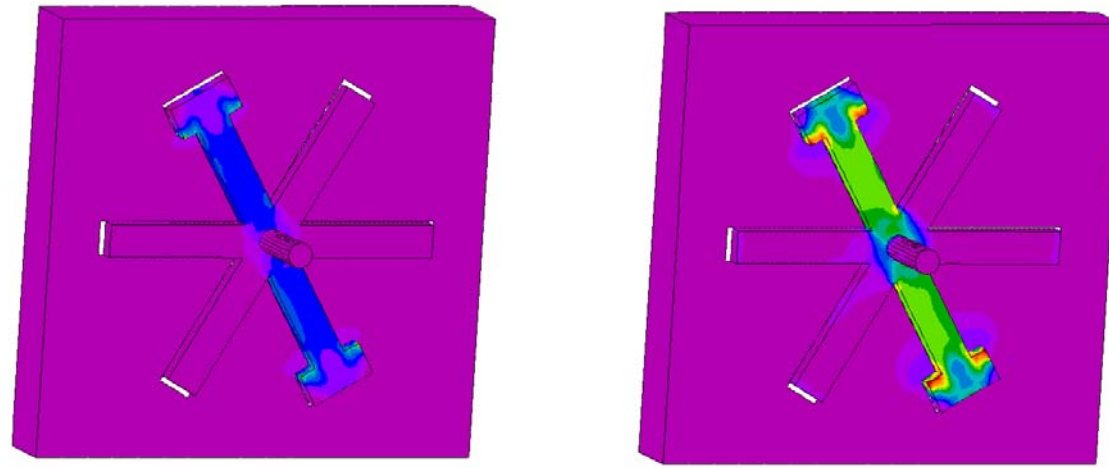
Figure 2: Effective Stress, Elastic Model (left) and Viscoplastic (right)
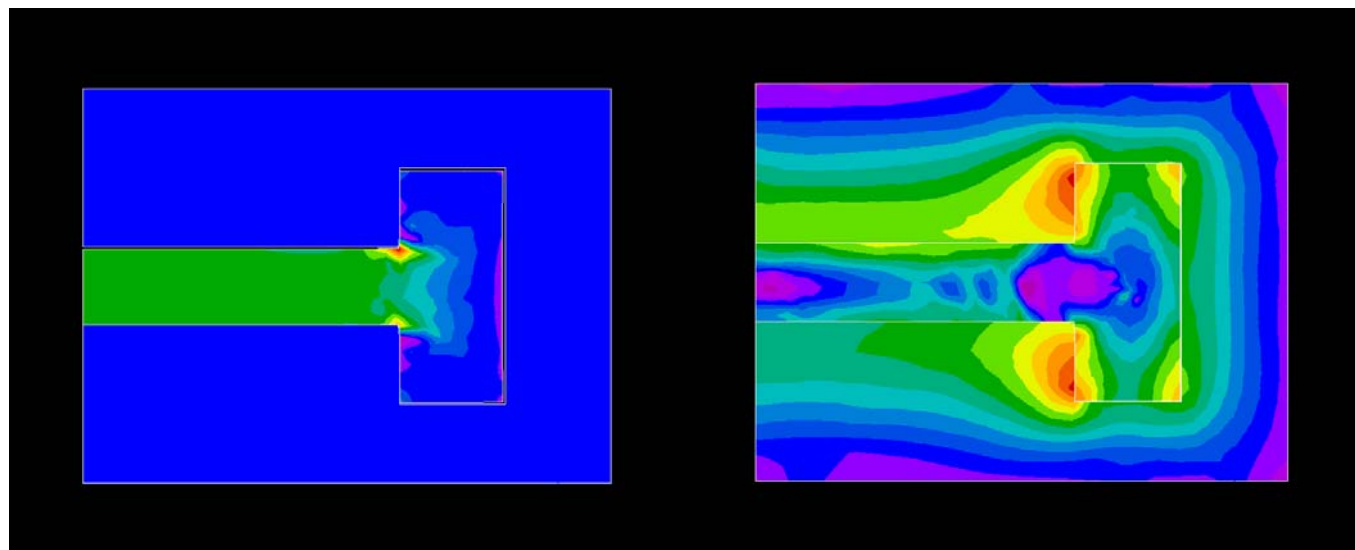
Figure 3: Principal Stress 1 and Heat Flux Contours
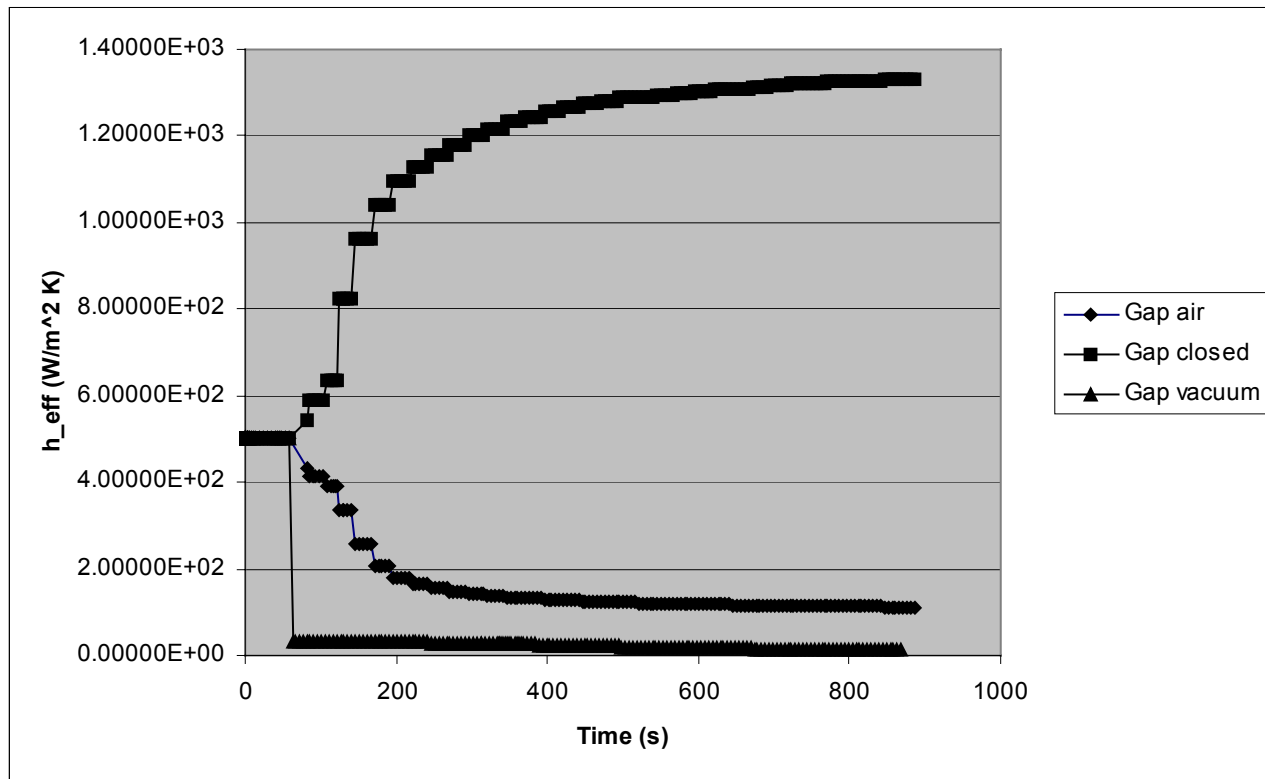
Figure 4: Interface heat transfer coefficients adjusted for mechanical contact
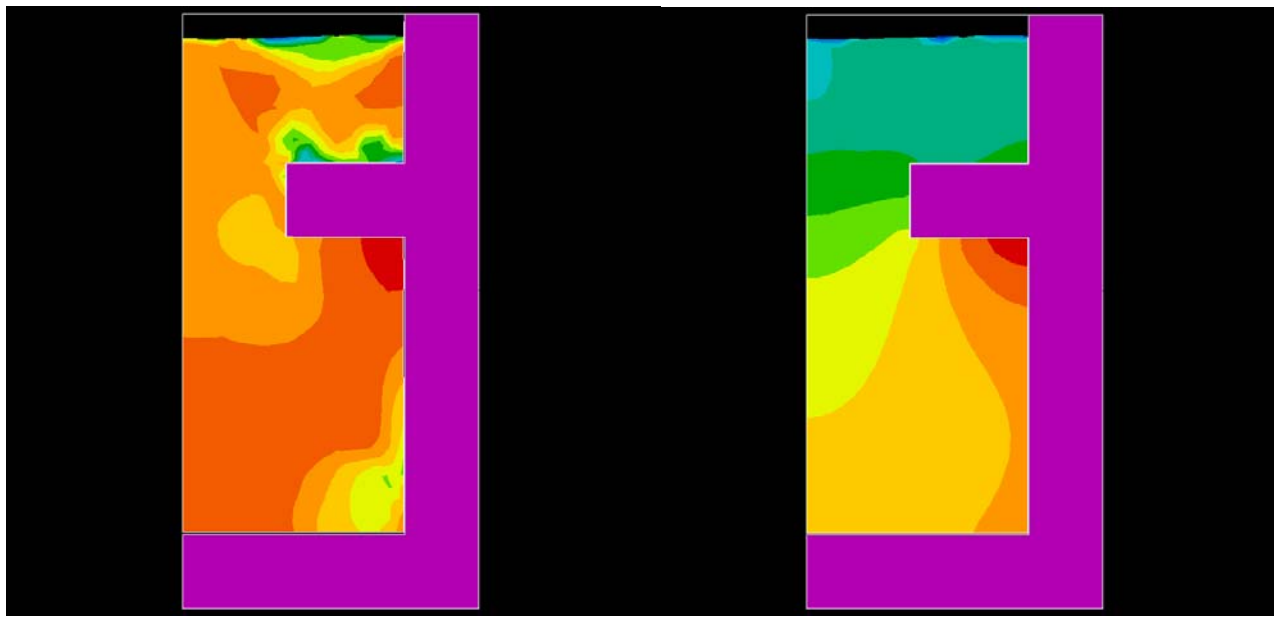
Figure 5: Treatment of Liquid Elements, Resulting Stress Contours
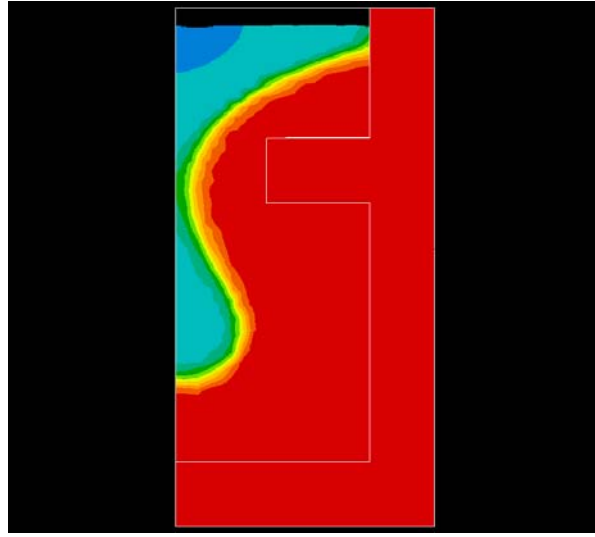
Figure 6: Fraction Solid Contours
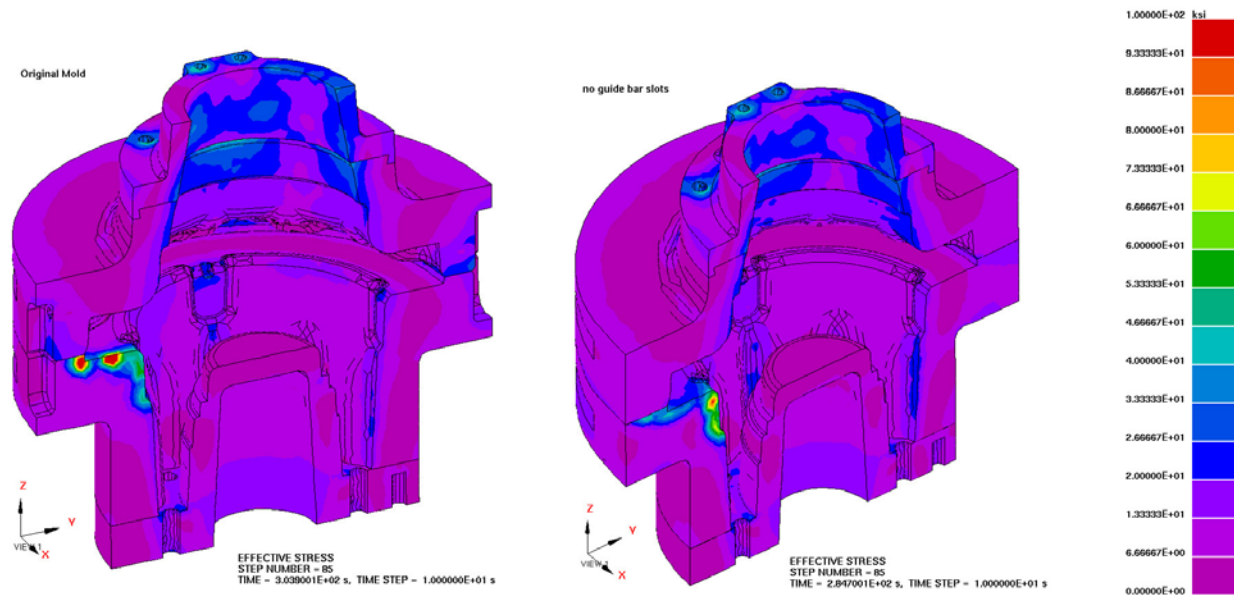
Figure 7. Stress contours in tilt pouring mold, before and after modification

References

1. P.Perzyna, 1966, 'Fundamental Problems in Viscoplasticity', Advance in Applied Mechanics, Vol.9, pp. 243-377.
2. P.J. Armstrong and C.O. Frederick, 1966, 'A mathematical representation of the multiaxial Bauschinger effect', General Electricity Generating Board, Report No. RD/B/N731, Bercley Nuclear Laboratories.
3. J.C. Simo and T.J.R. Hughes, 1998, Computational Inelasticity, Springer.
4. J.C. Simo and T.A. Laursen, 1992, 'An augmented Lagrangian treatment of contact problems involving friction', Comput. & Structures, Vol. 42, pp.97-116.
5. O.C. Zienkiewicz and R.L.Taylor, 1991, The Finite Element Method, Volume 2, McGraw-Hill.
6. ProCAST User Manual & Technical Reference, 1998.